Low temperature electrical transport properties of RuO$_2$ and IrO$_2$ single crystals

Low temperature electrical transport properties of RuO_2 and IrO_2 single crystals

J J Lin[1,2]**, S M Huang**[1]**, Y H Lin**[1]**, T C Lee**[1]**, H Liu**[3]**, X X Zhang**[3]**, R S Chen**[4] **and Y S Huang**[4]

[1] Institute of Physics, National Chiao Tung University, Hsinchu 300, Taiwan
[2] Department of Electrophysics, National Chiao Tung University, Hsinchu 300, Taiwan
[3] Department of Physics and Institute of Nano Science and Technology, The Hong Kong University of Science and Technology, Clear Water Bay, Kowloon, Hong Kong, People's Republic of China
[4] Department of Electronic Engineering, National Taiwan University of Science and Technology, Taipei 106, Taiwan

E-mail: jjlin@mail.nctu.edu.tw

Abstract

We have systematically measured the electrical transport properties of several RuO_2 and IrO_2 single crystals over a wide temperature range from 300 K down to 0.3 K to study the conduction mechanisms in these oxides. Our measured resistivities are in close agreement with the recent band-theory calculations for these materials. The characteristic temperatures for the acoustic-mode and optical-mode phonons are determined. Our measured magnetoresistances are positive and follow the Kohler rule, indicating that the transport properties of these oxides exhibit normal behaviour as described by the Boltzmann equation. In contrast, we do not find any signature of superconductivity down to 0.3 K, though the band-theory calculations predict a superconducting transition temperature of ∼5 K. Magnetization measurements suggest a very low level of paramagnetic impurities in our crystals.

1. Introduction

The electronic structures and electrical transport properties of the dioxides RuO_2 and IrO_2 have recently been extensively studied. For example, the band structures of these dioxides have been calculated by several authors [1–6], while the electrical transport properties have been explicitly calculated by Glassford and Chelikowsky [5]. Experimentally, the electronic and transport properties of these metals have also been investigated over the years [7–10]. It is often accepted that the current understanding of these materials is quite complete. In particular, the electrical resistivities of these materials between 20 and 1000 K have been

measured in [9] and recently been reanalysed in [5]. On the other hand, the resistivities and magnetoresistivities of these materials have never been measured down to liquid-helium and sub-kelvin temperatures.

According to the band-structure calculations of Glassford and Chelikowsky [5], the electrical resistivity of RuO_2 at not-too-high temperatures is comprised of two terms:

(1) the usual Bloch–Grüneisen contribution due to the coupling of electrons with acoustic-mode phonons (characterized by a coupling constant λ_{BG}); and
(2) an additional contribution due to the coupling of electrons with optical-mode phonons (characterized by a coupling constant λ_E).

In this work, we report our measurements of the resistivities and magnetoresistivities of several RuO_2 and IrO_2 single crystals over a wide temperature range from 300 K down to 0.3 K. These two materials are studied together, because they crystallize in the same rutile structure and reveal similar transport properties. By comparing our experimental results with the predictions of [5], we are able to extract the values of the relevant parameters λ_{BG}, λ_E and the Debye temperature (θ_D) of these materials.

2. Experimental method

Single crystals of RuO_2 and IrO_2 were grown by the method of chemical transport reaction in a flowing oxygen system as described previously [11, 12]. The gaseous oxide, RuO_3 or IrO_3, was formed by the reaction

$$M(\text{solid}) + \tfrac{3}{2}O_2 \rightarrow MO_3(\text{gas})$$
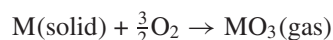
where M = Ru or Ir, when oxygen was passed over Ru (Ir) metal powder at a temperature of about 1200 °C (1250 °C) and at a flow rate of approximately 100 cm^3 min^{-1}. The volatile MO_3 gas then decomposed and crystallized into highly ordered single crystals of MO_2 at about 1000 °C. X-ray powder diffraction analysis was performed to establish the tetragonal rutile structure, and Laue backscattering was used to identify the growth habits.

Our samples were irregular in shape. For convenience in resistance and magnetoresistance measurements, we used thin slice-shaped and needle-shaped samples. Typical slices were ~1–2 mm wide and ~0.015–0.22 mm thick. Typical needles were ~0.1–0.2 mm in diameter. Four-probe electrical contacts were made with silver paste, and the typical distance between the voltage probes was ~0.5–1.7 mm. Standard four-probe resistances and magnetoresistances were measured using a Linear Research LR-700 resistance bridge and/or a Keithley 220 current source with a Keithley 182 nanovoltmeter. The resistivities of our samples were computed and estimated to be subject to an uncertainty of about 40–50%, due to the appreciable uncertainties in the dimensions of the samples. Roughly speaking, our room temperature resistivities are ~100 $\mu\Omega$ cm in RuO_2 and ~50–120 $\mu\Omega$ cm in IrO_2. On the other hand, the resistance ratio, $R(300\,\text{K})/R(4\,\text{K})$, for each sample can be measured very accurately. Our values are $R(300\,\text{K})/R(4\,\text{K}) = 81$–128 in RuO_2 and 224–826 in IrO_2. For this reason, table 1 lists only the values of $R(300\,\text{K})/R(4\,\text{K})$, but not the individual values of ρ, for each sample. It should be noted that our measured resistivities and resistance ratios are in reasonably good agreement with those previously reported by Ryden *et al* [8].

The resistance measurements of our samples were performed on a standard ^{4}He dipper and an Oxford Heliox ^{3}He cryostat. In the ^{4}He dipper, the temperature was monitored using a calibrated AlGaAs thermometer. In the Heliox ^{3}He refrigerator, a calibrated carbon glass thermometer was used for monitoring temperatures above 7 K, while a calibrated RuO_2 thermometer was used for monitoring temperatures below 7 K. The magnetoresistance
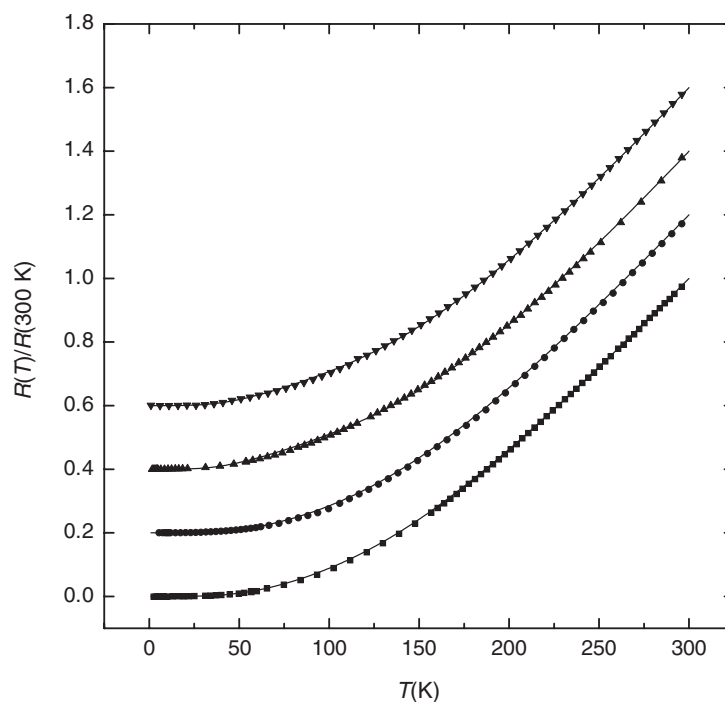
Figure 1. Normalized resistance $R(T)/R(300\text{ K})$ as a function of temperature for the (from the bottom up) RuO$_2$-C, RuO$_2$-A, IrO$_2$-A, and IrO$_2$-C single crystals. The symbols are the experimental data, and the solid curves are the theoretical fits to the sum of equations (1)–(3) as described in the text. For clarity, the data for RuO$_2$-A, IrO$_2$-A, and IrO$_2$-C have been shifted by +0.2, +0.4, and +0.6, respectively.

Table 1. Values of relevant parameters for RuO$_2$ and IrO$_2$ single crystals. The uncertainty in the fitted values of λ_{BG} and λ_E is ±10%, while the uncertainty in the fitted values of θ_D (θ_E) is ±5% (±3%).

Sample	$R(300\text{ K})/R(4\text{ K})$	λ_{BG}	λ_E	θ_D (K)	θ_E (K)
RuO$_2$-A	119	0.14	0.25	401	813
RuO$_2$-B	128	0.13	0.28	404	811
RuO$_2$-C	81	0.12	0.24	401	813
IrO$_2$-A	826	0.11	0.25	280	889
IrO$_2$-B	224	0.13	0.28	289	885
IrO$_2$-C	243	0.11	0.24	296	870
IrO$_2$-D	328	0.14	0.27	292	850

measurements were performed on an Oxford SM-4000 ^{4}He cryostat equipped with a 6 T split-coil superconducting magnet. The temperature was monitored with a calibrated carbon glass thermometer.

3. Results and discussion

Figure 1 shows the normalized resistances, $R(T)/R(300\text{ K})$, as a function of temperature for two RuO$_2$ and two IrO$_2$ single crystals. The symbols are the experimental data and the

solid curves are the band-theory calculations of [5]. This figure clearly demonstrates that the measured resistances are well described by the theoretical predictions. It should be noted that Ryden *et al* [8] have previously found that the resistivity in RuO_2 is essentially independent of the crystal orientation, i.e., their measured resistivities in the [100], [001], [011], and [111] directions are basically indistinguishable. Based on this observation, the orientation of our crystal with respect to the measuring current need not be specified. In practice, for all crystals, our measuring currents are essentially in the [001] direction.

In the theory of [5], the resistivity of RuO_2 is comprised of three terms. The first contribution is the usual Bloch–Grüneisen term due to the coupling of electrons with acoustic-mode phonons, and is given by

$$\rho_{BG}(T) = \frac{32\pi^2}{\hbar\Omega_p^2} k_B T \lambda_{BG} \left(\frac{T}{\theta_D}\right)^4 \int_0^{\theta_D/T} \frac{x^5 \, dx}{4\sinh^2(x/2)}, \tag{1}$$

where Ω_p is the plasma frequency. The second term is an additional contribution due to the coupling of electrons with optical-mode phonons (this term is important for transition-metal oxides which contain multi-atom bases), and is given by

$$\rho_E(T) = \frac{8\pi^2}{\hbar\Omega_p^2} k_B T \lambda_E \left[\frac{\theta_E/2T}{\sinh(\theta_E/2T)}\right]^2. \tag{2}$$

That is, in this theory, the optical-mode coupling term is treated using the Einstein approximation with a single phonon frequency corresponding to the energy $k_B\theta_E$, where k_B is the Boltzmann constant. The third contribution is due to the usual electron–electron scattering which depends on the square of the temperature, and can be written as

$$\rho_{ee}(T) = A_{ee}T^2, \tag{3}$$

where A_{ee} is a temperature independent parameter. The measured normalized resistivity, $\rho(T)/\rho(300\text{ K}) = R(T)/R(300\text{ K})$, can then be fitted to the sum of equations (1)–(3) with λ_{BG}, θ_D, λ_E, θ_E, and A_{ee} as adjusting parameters. For real single-crystalline samples having finite residual resistances, the third term, equation (3), is *negligible* if the measuring temperature is not extremely high (e.g., several hundred kelvins and higher)[5].

Table 1 lists the values of the fitting parameters for our samples. For comparison, Glassford and Chelikowsky obtained the values of $\lambda_{BG} \approx 0.14$, $\lambda_E \approx 0.33$, $\theta_D \approx 409$ K, and $\theta_E \approx 787$ K for RuO_2. Experimentally, the ratio of our fitted values of λ_{BG}/λ_E, which determines the relative contribution of the acoustic-mode phonon and optical-mode phonon terms, is ≈ 0.5 for both RuO_2 and IrO_2. It should be noted that the values of θ_D for RuO_2 reported in previous measurements were 650 ± 40 and 900 ± 50 K in [7] and [8], respectively. These previous values were clearly overestimated.

As for IrO_2, the values of θ_D previously reported in [7] (≈ 470 K) and [8] ($= 700 \pm 100$ K) are significantly higher than our result of ≈ 290 K (see table 1). Unfortunately, no band-structure calculations for the electronic and transport properties of IrO_2 are available in the literature.

In the presence of a magnetic field B and at liquid-helium temperatures, the magnetoresistances for all our RuO_2 and IrO_2 crystals reveal similar behaviour and are all positive. (In this work, we focus on the case where the magnetic field is applied perpendicular to the measuring current.) In low magnetic fields, the magnetoresistances vary quadratically with the field, as expected. In higher magnetic fields of the order of tens of kG, depending on temperature and the sample, the magnetoresistances increase somewhat linearly with

---

[5] In practice, the resistivity due to the electron–electron scattering in transition metals is of the order of $\rho_{ee} \sim (10^{-5}\text{ K}^{-2})T^2 \mu\Omega$ cm, where T is in kelvins, for example see [13].
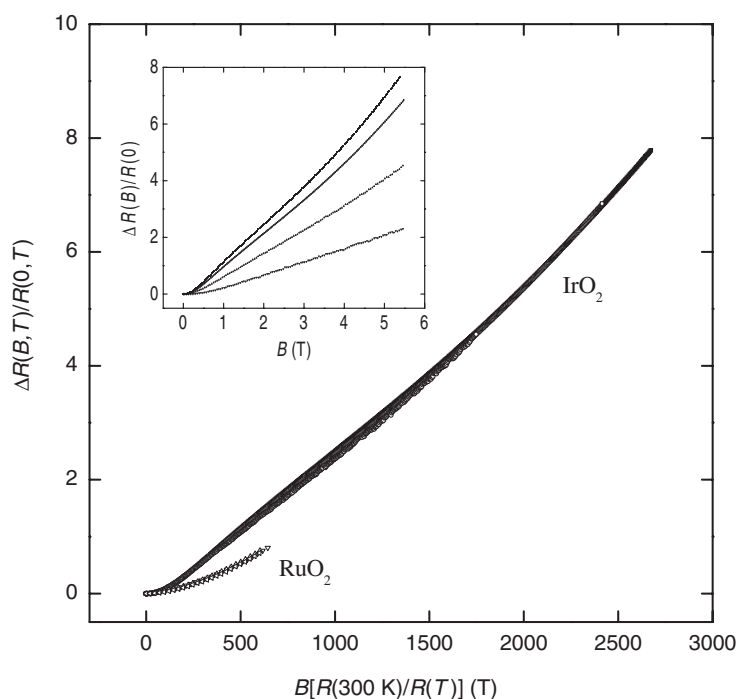
Figure 2. Normalized magnetoresistance $\Delta R(B, T)/R(0, T) = [R(B, T) - R(0, T)]/R(0, T)$ as a function of the normalized magnetic field $B[R(300\,\text{K})/R(T)]$ for the RuO$_2$-B single crystal at 10.0, 20.0, and 30.0 K, and the IrO$_2$-A single crystal at 6.0, 10.0, and 20.0 K. For each crystal, the normalized magnetoresistance obeys the Kohler rule and the magnetoresistances measured at different temperatures overlap closely and (the symbols) are indistinguishable. The inset shows the normalized magnetoresistance as a function of magnetic field for the IrO$_2$-A single crystal at four temperatures (from the top down): 4.2, 10.0, 20.0, and 30.0 K.

increasing field up to our highest measuring field of 5.5 T. The inset of figure 2 shows the magnetoresistances as a function of magnetic field for an IrO$_2$ crystal at four temperatures as indicated in the caption to figure 2. Quantitatively, a plot of the normalized magnetoresistance, $[R(B, T) - R(0, T)]/R(0, T)$, versus the normalized field, $B[R(300\,\text{K})/R(T)]$, indicates that the measured magnetoresistances closely obey the Kohler rule [14] below about 30 K. That is, for every sample, the normalized magnetoresistances measured at different temperatures scale with the normalized magnetic field. Above about 30 K, the contribution from the optical-mode term becomes non-negligible, and a small deviation from the Kohler rule is observed. The normalized magnetoresistances illustrating the Kohler rule for one representative IrO$_2$ and one RuO$_2$ single crystal measured at several temperatures are plotted in the main panel of figure 2. This observation of an 'orthodox' magnetoresistance phenomenon supports the Glassford–Chelikowsky prediction [5] that the transport properties of RuO$_2$ exhibit normal behaviour as described by the Boltzmann equation.

With the values of the electron–phonon coupling constants λ_{BG} and λ_{E} being determined, and assuming the renormalized Coulomb pseudopotential $\mu^* = 0.1$, one might be tempted to predict a superconducting transition temperature of $\sim$5 K in RuO$_2$ [5, 16]. To test this conjecture, we have performed careful resistance measurements down to 0.3 K. Figure 3 shows the normalized resistance, $R(T)/R(5\,\text{K})$, as a function of temperature for one IrO$_2$ and two RuO$_2$ crystals between 0.3 and 6 K. This figure clearly illustrates that the resistances
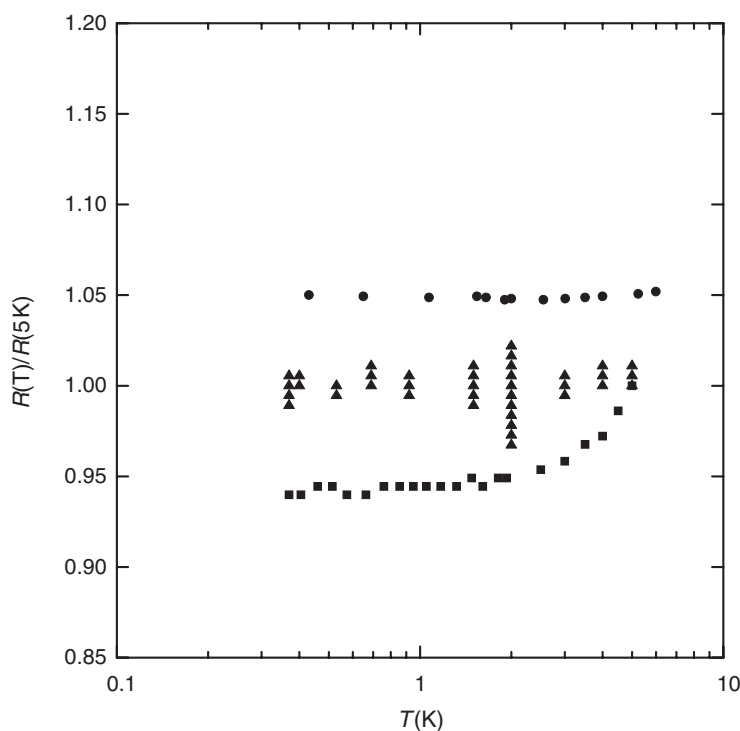
Figure 3. Normalized resistance $R(T)/R(5\,\mathrm{K})$ as a function of temperature for the RuO_2-B (circles), RuO_2-A (triangles), and IrO_2-B (squares) single crystals below 6 K. For clarity, the data for the RuO_2-B have been shifted by +0.05. The data for the RuO_2-A reflect the largest possible uncertainties in our measurements due to the smallness of the sample resistance.

remain constant down to 0.3 K, with no sign of an abrupt drop to a zero resistance for any sample. The finite residual resistance reflects the existence of a low concentration of defects or impurities in the samples. Thus, to clarify whether our crystals might contain a minute amount of magnetic impurities, we have performed magnetization measurements between 2 and 300 K, using a Quantum Design SQUID magnetometer. Our measured magnetizations above several tens of kelvins are consistent with previous results [15]. Below around 35 K, however, we found a slight increase in magnetization with decreasing temperature, indicating the presence of a low level of paramagnetic impurities in the crystals. Quantitatively, our measured low temperature magnetizations are well described by the Curie law from which an estimate of a magnetic impurity level of 20 ppm in both RuO_2 and IrO_2 could be inferred, if we assume that the paramagnetic impurities are mainly due to Fe^{3+} ions. This estimate is in satisfactory consistency with the spectrographic analysis of our starting Ru and Ir metals. Generally, a level of 20 ppm of magnetic impurities would barely suppress the superconducting transition [17], if such a transition does exist initially, as speculated in [5, 16]. Whether spin fluctuations or other detrimental mechanisms (e.g., strong electron–electron interactions) might play a role in suppressing superconductivity in RuO_2 deserves further study.

4. Conclusion

We have systematically measured the resistivities of several RuO_2 and IrO_2 single crystals over a wide temperature range from 300 to 0.3 K. Our results for the resistance as a function

of temperature agree well with the recent band-structure calculations. Our magnetoresistance measurements also demonstrate that the transport properties of these dioxides exhibit normal behaviour as described by the Boltzmann equation.

Acknowledgment

References

[1] Mattheiss L F 1976 *Phys. Rev.* B **13** 2433
[2] Sasaki T A and Soga T 1981 *Physica* B **111** 304
[3] Xu J H, Jarlborg T and Freeman A J 1989 *Phys. Rev.* B **40** 7939
[4] Glassford K M and Chelikowsky J R 1993 *Phys. Rev.* B **47** 1732
[5] Glassford K M and Chelikowsky J R 1994 *Phys. Rev.* B **49** 7107
[6] Yavorsky B Yu, Krasovska O V, Krasovskii E E, Yaresko A N and Antonov V N 1996 *Physica* B **225** 243
[7] Passenheim B C and McCollum D C 1969 *J. Chem. Phys.* **51** 320
[8] Ryden W D, Lawson A W and Sartain C C 1970 *Phys. Rev.* B **1** 1494
[9] Ryden W D, Reed W A and Greiner E S 1972 *Phys. Rev.* B **6** 2089
[10] Graebner J E, Greiner E S and Ryden W D 1976 *Phys. Rev.* B **13** 2426
[11] Huang Y S and Liau P C 1987 *Chin. J. Phys.* **25** 232
[12] Reames F M 1976 *Mater. Res. Bull.* **11** 1091
[13] Dugdale J S 1977 *The Electrical Properties of Metals and Alloys* (London: Edward Arnold)
[14] Ziman J M 1960 *Electrons and Phonons* (Oxford: Clarendon)
[15] Fletcher J M, Gardner W E, Greenfield B F, Holdoway M J and Rand M H 1968 *J. Chem. Soc.* A 653
     Cotton F A and Mague J T 1966 *Inorg. Chem.* **5** 317
     Guthrie A N and Bourland L T 1931 *Phys. Rev.* **37** 303
[16] Allen P B 2000 *Handbook of Superconductivity* ed C P Poole Jr (New York: Academic)
[17] Riblet G 1971 *Phys. Rev.* B **3** 91
     Gladstone G, Jensen M A and Schrieffer J R 1969 *Superconductivity* ed R D Parks (New York: Dekker)